Korean J. Chem. Eng., 33(6), 1971-1976 (2016)
DOI: 10.1007/s11814-016-0037-2

pISSN: 0256-1115
eISSN: 1975-7220

Extremely flexible organic-inorganic moisture barriers

Se Hee Lim, Seung-Woo Seo, Haksoo Lee, Heeyeop Chae, and Sung Min Cho†

School of Chemical Engineering, Sungkyunkwan University, Suwon 16419, Korea
(*Received 10 September 2015 • accepted 1 February 2016*)

Abstract−Organic/inorganic multilayer structures were fabricated for extreme flexibility as well as enhanced moisture-barrier property. The organic and inorganic layers for the structures were formed by plasma polymerization and atomic layer deposition, respectively. The layers were grown alternately to form the organic/inorganic multilayer structures on a plastic substrate. To accomplish extreme flexibility of the barriers, ultra-thin aluminum oxide layers were grown by the atomic layer deposition and sandwiched by a flexible plasma-polymer layer. The moisture-barrier films were then confirmed to retain the initial barrier property even after 10,000 times of bending at a radius as small as 3 mm when the barrier structure was located at a neutral plane.

Keywords: Moisture Barrier, Atomic Layer Deposition, Plasma Polymerization, Bending Radius

INTRODUCTION

Organic light-emitting diode (OLED) requires thin-film encapsulation for the blockage of ambient moisture, which could damage a low work-function metal cathode or organic layers in the device. To realize a flexible OLED device, the thin-film encapsulation layer should not only be a good moisture barrier but also flexible. For thin-film encapsulation, aluminum oxide (AlO_x) has been the material of choice since the films grown by atomic layer deposition (ALD) have been shown to provide superior protection from moisture degradation of OLEDs [1-6]. However, the ALD-grown AlO_x thin films have intrinsically limited flexibility. The critical tensile strain of 20 nm-thick AlO_x thin film is known to be about 1.16% [7], which corresponds to a critical bending radius of 5.3 mm.

To provide a thin AlO_x layer with better bending ability, it is advantageous for the layer to be sandwiched by a flexible polymer layer. This hybrid or multilayer approach not only improves the bending property, but also lowers water vapor transmission rate (WVTR) values, by making the moisture penetration paths through the defects in the sandwiched AlO_x layers much longer and tortuous. The WVTR is a moisture flux through a moisture barrier layer with a general unit of $gH_2O/m^2/day$. For the flexible polymer layer, we utilized plasma-polymerized organic layers (plasma polymers), which can be grown in a plasma-enhanced chemical vapor deposition (PECVD) reactor with organic monomer sources.

Plasma polymerization is becoming increasingly popular due to its simplicity and ease of operation at room temperature. The fragmentation of the organic monomer sources in the plasma results in the formation of plasma-polymer films on a substrate surface. The advantageous features of plasma polymers include a more random structure than conventional polymers, extensive cross-linking, covalent bonding to substrates, and easy thickness control in the range from nanometers to micrometers. Therefore, the films produced by plasma polymerization are usually insoluble, pinhole-free, and adhere well to substrates. Many simple monomer precursors are readily polymerized by this method. Common monomers such as thiophene [8,9], pyridine [10,11], acrylonitrile [12], furan [13], styrene [14], n-hexane [15], and hexamethyldisiloxane (HMDSO) [16-18] have been used for the plasma polymerization.

To check the applicability of the organic/inorganic multilayer for flexible thin-film encapsulation of OLEDs, the moisture-barrier property and flexibility of the multilayer structure should be investigated. The moisture-barrier property and flexibility are often measured by a calcium (Ca) test and bending test, respectively [19, 20]. The Ca test measures WVTR values of the multilayer structures. By measuring the WVTR change of a multilayer structure before and after repeated bending cycles at a bending radius, we can quantify the flexibility of a multilayer structure as the bending radius. The organic/inorganic multilayer structure has been shown effective for flexible thin-film encapsulation of OLEDs [19].

In this study, we investigated the ALD of AlO_x and the plasma polymerization of three distinctly different monomers: an organometallic HMDSO, a ring-type furan, and an aliphatic n-hexane. The moisture-barrier property of single-layer plasma polymers and multilayer structures of AlO_x/plasma polymer was reported. This study also reports how we could maximize the flexibility of the structures by reducing the AlO_x thickness or putting the structures in a neutral plane.

EXPERIMENTAL PROCEDURE

For the ALD deposition of AlO_x layers, an in-house designed and built deposition equipment was used, with two precursors of trimethyl aluminum (TMA) and water, which were vaporized at 5 °C and room temperature, respectively. The substrate was polyethylene naphthalate (PEN) film (Dupont Teonex, Q65FA). The substrate surface with 0.7 nm root-mean-square roughness was

†To whom correspondence should be addressed.
E-mail: sungmcho@skku.edu

ultrasonically cleaned with acetone, followed by isopropyl alcohol, methanol, and finally deionized water for 20 min. each. The deposition was carried out at the substrate temperature of 80 °C. At first, water was introduced into the deposition chamber for 2 s to treat the PEN film surface. Then the chamber and precursor lines were purged out with argon (Ar) gas for 10 s until the chamber pressure reached 3×10^{-2} torr. The actual growth cycle of AlO_x was TMA injection for 2 s, purging with Ar for 10 s, water injection for 2 s, and purging water with Ar for 10 s. Each cycle produced a 1.1 Å-thick AlO_x layer on average, at that temperature.

Plasma polymerization involved using an inductively-coupled plasma reactor comprised of a coiled Pyrex tubular chamber, 60 cm long and 8 cm in diameter. The chamber was evacuated down to 1.0×10^{-3} torr prior to the supply of monomers. The three monomers, HMDSO, n-hexane and furan, were supplied with Ar carrier gas. The flow rates of monomer and carrier gas were set to 10 and 30 sccm, respectively, and the radio-frequency input power was changed from 50 W to 150 W. The polymerization was monitored by measuring the Fourier transform infrared (FTIR) spectra of both the three monomers and the plasma-polymerized layers derived from the monomers.

To prepare organic/inorganic multilayer structures, plasma polymers and AlO_x layers were grown sequentially and alternately. Prior to the ALD growth of the AlO_x layer on a plasma-polymer surface, oxygen-plasma treatment was carried out to form hydroxyl groups on the plasma-polymer surface. The growth of the multilayer structure was confirmed by measuring the water-contact angle on each surface produced after a separate growth step and by taking cross-sectional TEM images of the final structure produced after the full growth procedure.

The moisture-barrier performance of the prepared multilayer structures was determined by an electrical Ca test using a 200 nm-thick Ca layer with an area of 1 cm×1 cm. For the test, the Ca layer was deposited on a glass substrate such that it was connected to two aluminum electrical leads. The Ca layer was then covered with barrier-deposited PEN film, the edges of which were sealed with a UV-curable epoxy resin (UV resin ZNR 5570 from Nagase & Co., Ltd. Japan). Detailed information of the Ca test procedure can be found in the literature [20]. During the Ca test measurement, electrical conductance through the Ca layer decreased as the Ca was oxidized by moisture permeated through the barrier film. All Ca tests were conducted at 85 °C and 85% relative humidity (RH) to accelerate the measurements. To confirm the water permeation through the edge-sealing epoxy, we fabricated a Ca-test sample encapsulated with glass. The sample endured 130 h until complete loss of the Ca conductance in the acceleration condition of 85 °C and 85% RH. This result indicates that moisture penetrated through the edge-sealing epoxy but not through the glass. The measured time in the Ca test in this study was always less than 30 h at the measurement condition, which means that negligible water permeated through the edge-sealing epoxy compared to that through the barrier film. For the Ca test measurement, four samples with an identical barrier structure were prepared and tested at the same time to check the reproducibility of the test. The multiple Ca tests of a barrier structure produced almost similar results and with the observation we confirmed the reproducibility of our Ca test.

The bending test was carried out with in-house designed equipment under ambient conditions. The bending radius was varied from 20 mm to 3 mm and the bending cycle was fixed at 10,000 times for all measurements. For the test, samples were at least 8 cm long, clamped at both ends, and allowed up to a 2 cm bending

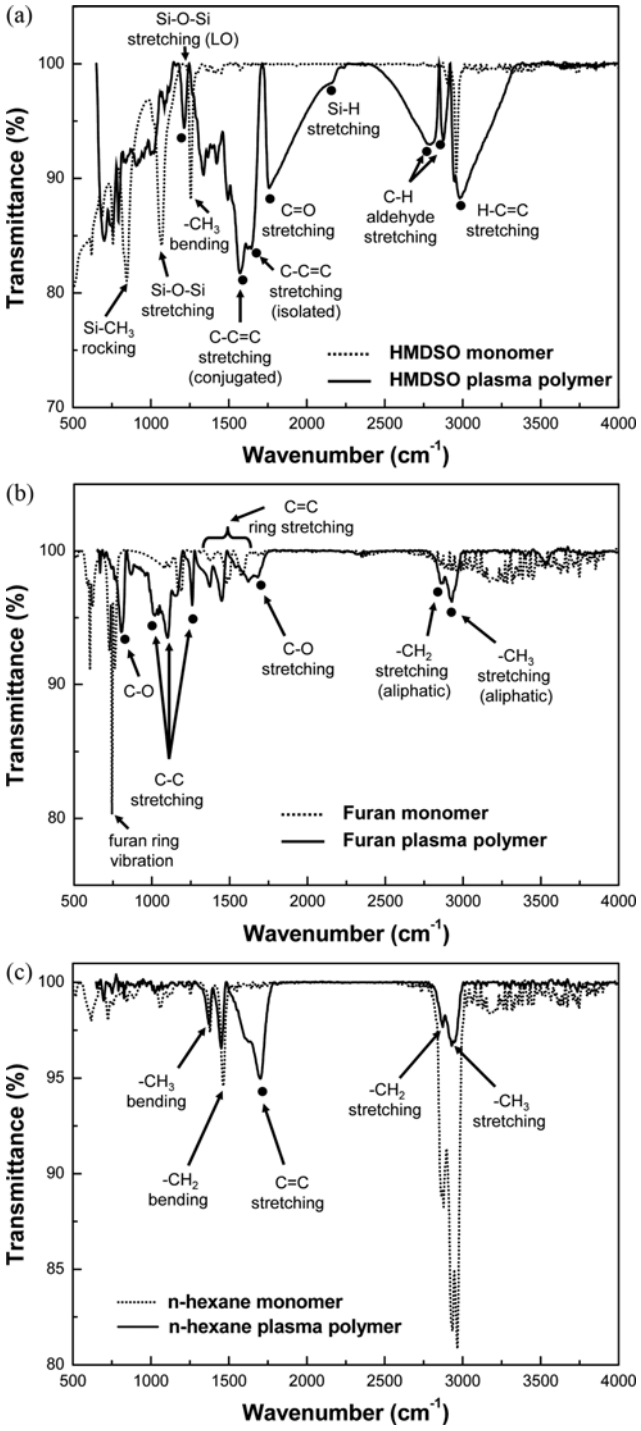

Fig. 1. FTIR spectra of (a) HMDSO monomer and the plasma polymer derived from HMDSO; (b) furan monomer and the plasma polymer derived from furan; (c) n-hexane monomer and the plasma polymer derived from n-hexane.

radius. The bending radius was defined at the center of the length of the substrate and given by the reciprocal of the curvature of the substrate computed by the sinusoidal bent shape of the substrate [21].

RESULTS AND DISCUSSION

The FTIR transmittance spectrum of organometallic HMDSO monomers in Fig. 1(a) shows well-resolved characteristic peaks for the functional groups in HMDSO molecules. After the plasma polymerization of the monomers in Ar plasma at 150 W, a few characteristic peaks disappeared and new peaks were generated due to the polymerization, as shown in the figure. The absorption intensities of the characteristic peaks assigned to Si-CH_3 and Si-O-Si decreased significantly after the polymerization. Instead, new characteristic peaks assigned to carbon double bonds appeared in high intensities as the result of the plasma polymerization. The characteristic peaks at 1,600-1,800 cm^{-1} were assigned to an isolated or conjugated C=C stretching and a C=O stretching [22]. The peaks appeared even at a lower plasma power of 50 W and the absorption intensity increased as the plasma power increased to 150 W. The appearance of C=C bonds proves the polymerization of HMDSO to form a plasma-polymer layer.

Ring-type furan monomers were polymerized in Ar plasma. Comparison of the FTIR spectra of the monomer furan and the polymer furan in Fig. 1(b) reveals that the ring stretching vibrations are retained in both the spectra in the region of 1,370-1,630 cm^{-1}, even though the characteristic peaks are shifted a little and the ring does not undergo any rupture in the plasma polymerization. However, the additional intense peaks (1,120 and 1,250 cm^{-1}) that were observed in the plasma-polymer spectrum were attributed to C-C stretching vibrations. The three peaks (1,120, 1,136, and 1,250 cm^{-1}) may be due to Fermi resonance, due to additional C-C bonds created in the process of polymerization. In electrochemically polymerized thiophene, which has a very similar structure, similar C-C stretching vibrations have been reported in this region [23]. These observations suggest that the plasma polymerization of furan has taken place via hydrogen abstraction. Even though plasma polymerization seldom occurs through hydrogen abstraction [24], these observations suggest a tentative structure of polyfuran generated by the plasma polymerization of furan [25].

The FTIR spectrum of n-hexane is rather simple, as shown in Fig. 1(c), due to its simple molecular structure. After plasma polymerization of n-hexane, a characteristic peak around 1,700 cm^{-1} appeared, which was assigned to C=C stretching vibrations and hence evidenced the polymerization of n-hexane.

Electrical Ca tests were carried out with the three different plasma polymers of the same thickness of 1 μm. As shown in Fig. 2, all the plasma-polymer layers on PEN substrates took longer time for Ca to be completely oxidized with moisture permeated at 85 °C and 85% RH than the time in case of a bare PEN substrate. The longer time corresponds to the better moisture barrier property because a longer time is required for the complete oxidation of an amount of Ca with a better barrier. Among the three plasma polymers we tested, the polymer derived from n-hexane showed the best moisture-barrier performance. Based on this result, the n-hexane plasma polymer was chosen for the organic layer in the organic/inorganic multilayer flexible barrier.

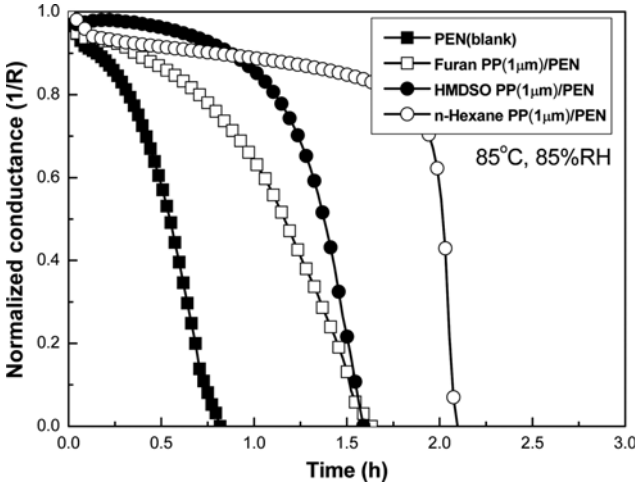

Fig. 2. Electrical Ca test results of a bare PEN substrate and plasma polymers on the substrate.

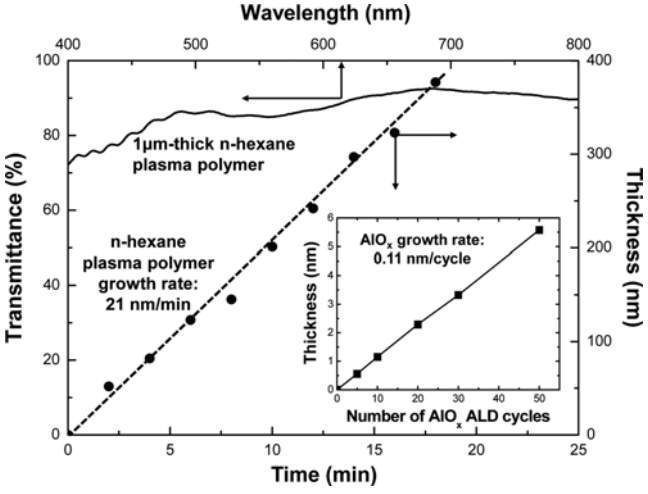

Fig. 3. The optical transmittance and growth rate of the plasma polymer derived from n-hexane. Inset shows the ALD growth rate of AlO_x.

The optical transmittance and growth rate of the plasma polymer are shown in Fig. 3. The film shows transmittance higher than 80% in the visible region with a thickness of 1 μm. The thickness of the plasma polymer increased linearly with increasing growth time. The growth rate was 21 nm/min at a plasma power of 50 W. The root-mean-square roughness of the plasma-polymer surface was 2.1 nm, even though it is not shown here. On the other hand, the ALD growth rate of AlO_x was 0.11 nm/cycle at a growth temperature of 80 °C, as shown in the inset of Fig. 3.

The water contact angle was measured at the surfaces of ALD-grown AlO_x and n-hexane plasma polymer. As shown in Fig. 4, the contact angles at the AlO_x and plasma polymer surfaces were 22° and 87°, respectively. To fabricate organic/inorganic multilayer structures consecutively, the plasma-polymer surface was treated with oxygen plasma prior to the ALD deposition of AlO_x to form hy-

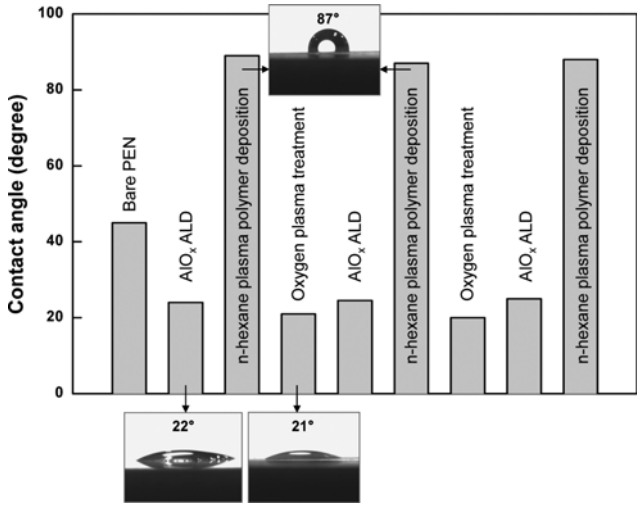

Fig. 4. Cyclic changes of water contact angle after each process step for an organic-inorganic multilayer structure.

droxyl groups on the surface. After the oxygen plasma treatment, the contact angle dropped significantly to 21°. By measuring the change in the contact angle after each processing step in the first two cycles, we confirmed the cyclic growth of organic/inorganic multilayer structures.

We fabricated a 20-dyad organic/inorganic multilayer structure composed of two-cycle ALD-grown AlO_x and 30 nm-thick plasma polymer. Here, a dyad means a pair of organic and inorganic layers. As shown in the cross-sectional TEM images in Fig. 5(a), the two-cycle-grown AlO_x layers form continuous layers between plasma-polymer layers. It has been reported [26] that an initial nucleation period exists prior to linear ALD growth on various polymer substrates. The nucleation and growth model for AlO_x ALD on low-density polyethylene substrate explains that the injected TMA reactant diffuses into the near-surface region of the polymer and is retained by being adsorbed at the initial stage of AlO_x ALD. During the first 10-15 cycles of successive TMA and water exposure, chemical reactions between TMA and water form small AlO_x clusters in the near-surface region and these AlO_x clusters grow to form a continuous AlO_x layer [26]. Unlike the nucleation and growth model, however, only two cycles of AlO_x ALD produced a continuous layer on the plasma polymer surface in this study. We consider that it is because the surface hydroxyl groups formed intentionally by the oxygen-plasma treatment of a dense plasma-polymer surface facilitated the AlO_x growth. As shown in Fig. 5(a), 20 continuous layers of AlO_x were clearly observed between plasma-polymer layers. The thickness of each AlO_x layer was around 1 nm, which was thicker than that expected with the linear growth rate (2.2 Å for two growth cycles) of our AlO_x ALD. It seems to be due to the surface roughness of the plasma polymer. In Fig. 5(b), mapping images of carbon and aluminum elements are shown.

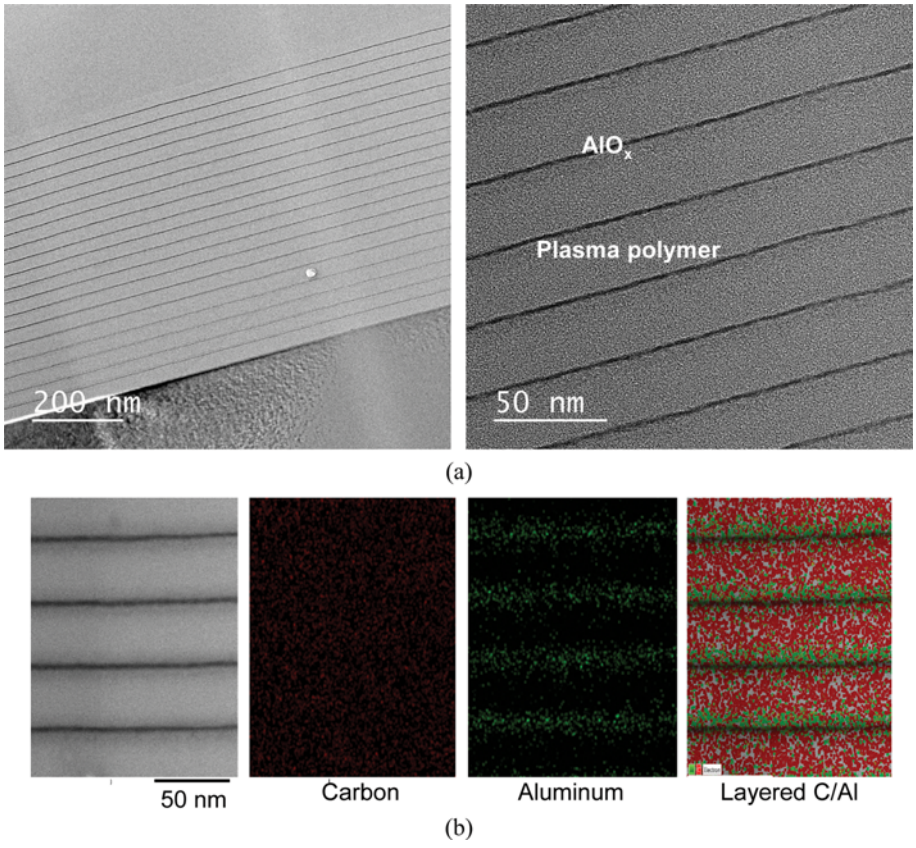

Fig. 5. (a) Cross-sectional transmission electron microscopy images of 20-dyad AlO_x/plasma polymer multilayer barrier; (b) element mapping images.

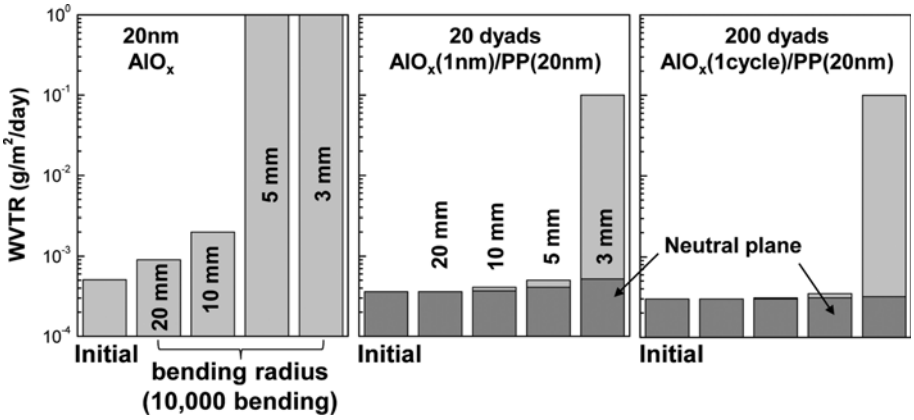

Fig. 6. The changes in WVTR of three different structures after 10,000 times of bending with four different bending radii.

Fig. 6 shows the bending property of organic/inorganic multilayer structures. An ALD-grown 20 nm-thick AlO_x on the PEN substrate showed an initial WVTR value of 5×10^{-4} g/m^2/day at ambient condition. A few organic/inorganic multilayer structures with the same total AlO_x thickness (20 nm) were formed to compare their barrier property and flexibility with the pure inorganic AlO_x structure. As shown in the figure, the initial WVTR values of the multilayer structures were found lower than that of the pure AlO_x, due to two possible reasons of the addition of plasma-polymer layers or the creation of tortuous path for moisture permeation in the multilayer structures. The WVTR of the pure AlO_x barrier tends to increase as the bending radius decreases from 20 mm to 3 mm. In all bending tests, the total number of bending cycles was fixed to 10,000. When the inorganic barrier was bent with a radius smaller than 5 mm, it lost the barrier property completely, and its WVTR turned out to that of the bare PEN substrate. However, the WVTR of the other two multilayer structures did not increase appreciably until the bending radius reached 3 mm, at which their WVTR increased abruptly. To enhance the moisture-barrier property of the multilayer structures further, we fabricated PEN film/multilayer barrier/PEN film so that a multilayer barrier was located at a neutral stress plane. For the structures, we attached a PEN film on the multilayer structures using an UV-curable resin. As shown in Fig. 6, the multilayer barriers at a neutral plane did not lose their moisture-barrier property even with a bending radius as small as 3 mm. Note that one cycle ALD growth of AlO_x could produce only 0.11 nm-thick layer, but the ultra-thin layer seems to work as a moisture barrier because it is continuous.

CONCLUSIONS

Organic/inorganic multilayer structures were fabricated for extreme flexibility as well as enhanced moisture-barrier property. The best structure retained the initial 3×10^{-4} g/m^2/day WVTR even after 10,000 times of bending at a radius as small as 3 mm when the structure was located at a neutral plane. We found that an ultra-thin AlO_x layer less than 1 nm thickness could be grown by ALD on a plasma-polymer surface and showed enhanced moisture-barrier property by the construction of multi-dyad structures with a plasma polymer. The extremely flexible organic/inorganic multilayer structures can be utilized as a thin-film encapsulation layer for flexible OLEDs.

ACKNOWLEDGEMENTS

This research was supported by the National Research Foundation of Korea (NRF) grant funded by the Korea government (MSIP) (NRF-2014R1A2A1A11052847).

REFERENCES

1. P. F. Carcia, R. S. McLean and M. H. Reilly, *Appl. Phys. Lett.*, **97**, 221901 (2010).
2. J. Meyer, H. Schmidt, W. Kowalsky, T. Riedl and A. Kahn, *Appl. Phys. Lett.*, **96**, 243308 (2010).
3. T. Riedl, T. Winkler, H. Schmidt, J. Meyer, D. Schneidenbach, H.-H. Johannes, W. Kowalsky, T. Weimann and P. Hinze, *IEEE Int. Reliab. Phys. Symp.*, Anaheim (USA), 327 (2010).
4. M. D. Groner, S. M. George, R. S. McLean and P. F. Carcia, *Appl. Phys. Lett.*, **88**, 051907 (2006).
5. A. A. Dameron, S. D. Davidson, B. B. Burton, P. F. Carcia, R. S. McLean and S. M. George, *J. Phys. Chem. C*, **112**, 4573 (2008).
6. P. F. Carcia, R. S. McLean, M. H. Reilly, M. D. Groner and S. M. George, *Appl. Phys. Lett.*, **89**, 031915 (2006).
7. S.-H. Jen, J. A. Bertrand and S. M. George, *J. Appl. Phys.*, **109**, 084305 (2011).
8. H. Goktas, F. G. Ince, A. Iscan, I. Yildiz, M. Kurt and I. Kaya, *Synth. Met.*, **159**, 2001 (2009).
9. P. Giungato, M. C. Ferrara, F. Musio and R. d'Agostino, *Plasmas and Polymers*, **1**, 283 (1996).
10. K. Hozumi, K. Kitamura, H. Hashimoto, T. Hamaoka, H. Fujisawa and T. Ishizawa, *J. Appl. Polym. Sci.*, **28**, 1651 (1983).
11. N. V. Bhat and D. J. Upadhyay, *Plasmas and Polymers*, **8**, 99 (2003).
12. Z. Jiang, Y. Meng, Z.-J. Jiang and Y. Shi, *Surf. Rev. Lett.*, **16**, 297 (2009).
13. M. C. Jobanputra, M. F. Durstock and S. J. Clarson, *J. Appl. Polym. Sci.*, **87**, 523 (2002).
14. A. J. Choudhury, J. Chutia, S. A. Barve, H. Kakati, A. R. Pal, Jagannath, N. Mithal, R. Kishore, M. Pandey and D. S. Patil, *Prog. Org.*

Coat., **70**, 75 (2011).
15. R. H. Pedersen, D. J. Scurr, P. Roach, M. R. Alexander and N. Gadegaard, *Plasma Process. Polym.*, **9**, 22 (2012).
16. J. Fang, H. Chen and X. Yu, *J. Appl. Polym. Sci.*, **80**, 1434 (2001).
17. K. Li, O. Gabriel and J. Meichsner, *J. Phys. D: Appl. Phys.*, **37**, 588 (2004).
18. P. Mandlik, J. Gartside, L. Han, I.-C. Cheng, S. Wagner, J. A. Silvernail, R.-Q. Ma, M. Hack and J. J. Brown, *Appl. Phys. Lett.*, **92**, 103309 (2008).
19. S.-W. Seo, H. Chae, S. J. Seo, H. K. Chung and S. M. Cho, *Appl. Phys. Lett.*, **102**, 161908 (2013).
20. S.-W. Seo, E. Jung, H. Chae and S. M. Cho, *Org. Electron.*, **13**, 2436 (2012).
21. S.-I. Park, J.-H. Ahn, X. Feng, S. Wang, Y. Huang and J. A. Rogers, *Adv. Funct. Mater.*, **18**, 2673 (2008).
22. B. Despax and P. Raynaud, *Plasma Process. Polym.*, **4**, 127 (2007).
23. K. Kaneto, K. Yoshino and Y. Inuishi, *Solid State Comm.*, **46**, 389 (1983).
24. H. Yasuda, *Plasma polymerization,* Academic Press, New York (1985).
25. A. Gok and L. Oksuz, *J. Macromol. Sci., Part. A: Pure Appl. Chem.*, **44**, 1095 (2007).
26. C. A. Wilson, R. K. Grubbs and S. M. George, *Chem. Mater.*, **17**, 5625 (2005).